[27] Fujikake K., Li B., Soeun S., 2009, "Impact response of reinforced concrete beam and its analytical evaluation," Journal of Structural Engineering, 135(8), 938-950.

[28] Pham T.M., Hao H., 2016, "Prediction of the impact force on reinforced concrete beams from a drop weight," Advances in Structural Engineering, 19(11), 1710-1722.

[29] Gholipour G., Zhang C., Mousavi A.A., 2018, "Effects of axial load on nonlinear response of RC columns subjected to lateral impact load: Ship-pier collision," Engineering Failure Analysis, 91, 397-418.

[30] Do T.V., Pham T.M., Hao H., 2018, "Numerical investigation of the behavior of precast concrete segmental columns subjected to vehicle collision," Engineering Structures, 156, 375-393.

[31] Hallquist J.O., 2007, "LS-DYNA keyword user's manual", Livermore Software Technology Corporation, 970, 299-800.

[32] Hao Y., Hao H., 2014, "Influence of the concrete DIF model on the numerical predictions of RC wall responses to blast loadings," Engineering Structures, 73, 24-38.

[33] Malvar L.J., Crawford J.E., 1998, "Dynamic increase factors for steel reinforcing bars [C].", The Twenty-Eighth DoD Explosives Safety Seminar Held, Orlando, USA.

[34] Kishi N., Mikami H., 2012, "Empirical formulas for designing reinforced concrete beams under impact loading," ACI Structural Journal-American Concrete Institute, 109(4), 509.

[35] Zhao L., Bi K., Hao H., Li X., 2017, "Numerical studies on the seismic responses of bridge structures with precast segmental columns," Engineering Structures, 151, 568-583.

[36] ACI Committee 318, 2008, "Building code requirements for structural concrete (ACI 318-08) and commentary (ACI318R-08)", American Concrete Institute, Farmington Hills, MI.

# Damage Accumulation Comparison of Fiber-Reinforced Concrete Using Repeated Drop Impact Testing

Andrew D. Sorensen, Robert J. Thomas, Ryan Langford and Abdullah Al-Sarfin

**Synopsis:** The impact resistance of concrete is becoming an increasingly important component of insuring the durability and resilience of critical civil engineering infrastructure. Design engineers are not currently able to use impact resistance as a performance-based specification in concrete due to a lack of a reliable standardized impact test for concrete. An improved method of the ACI standard, ACI 544.2R-89 Measurement of Properties of Fiber Reinforced Concrete, is developed that provides a resistance curve as a function of impact energy and number of blows (N) to failure. The curve provides information about the life cycle (N) under repeated sub-critical impact events and an estimate of the critical impact energy (where N=1), whereas the previous method provided only a relative value. The generated impact-fatigue curve provides useful information about damage accumulation under repeated impact events and the effectiveness of the fiber-reinforcement. In this paper, the improved method is demonstrated for three fiber types: steel, copolymer polypropylene, and a monofilament polypropylene. Additionally, the analytical solution for the specimen geometry is given as well as the theoretical considerations behind the development of the impact-life curve. The use of a specimen geometry provides a path to generalize the test results to full-scale structures.

**Keywords:** drop-weight impact, damage prediction, fiber reinforced concrete, impact testing standards

ACI member **Andrew D. Sorensen** is an Assistant Professor in the Department of Civil and Environmental Engineering at Utah State University, Logan, UT. He is an associate member of ACI Committees 370 (Blast and Impact Load Effects) and 348 (Structural Reliability and Safety). His research interests encompass the reliability of materials and structures under extreme and multi-hazard loading scenarios.

ACI member **Robert J. Thomas** is an Assistant Professor in the Department of Civil and Environmental Engineering at Clarkson University, Potsdam, NY. He is a voting member of ACI Committees 123 (Research and Current Developments) and 242 (Alternative Cements) and an associate member of Committee 239 (Ultra-High-Performance Concrete). His research interests include alternative cements, advanced cementitious composites, damage mechanics, and sustainability.

ACI student member **Ryan "Nick" Langford** is a Graduate Student in the Department of Civil and Environmental Engineering at Utah State University, Logan, UT.

ACI student member **Abdullah Al Sarfin** is a Graduate Student in the Department of Civil and Environmental Engineering at Utah State University, Logan, UT.

## INTRODUCTION

The impact resistance of concrete is becoming an increasingly important component of insuring the durability and resilience of critical civil engineering infrastructure. Design engineers are not currently able to use impact resistance as a performance-based specification in concrete due to a lack of a reliable standardized impact test for concrete. Many studies have been carried out to characterize the impact resistance and energy absorption capacity of plain and fiber-reinforced concrete. These studies have attempted to quantify the effect of different types of fibers, rebar, silica fume, water-cement ratio, loading rates, types of aggregates, among other parameters [1–10]. It is reported that the combination of steel fiber and steel rebar provides better positive composite effect and improves impact resistance compared to the concrete having either steel fiber or steel rebar [5]. Zhang et al. investigated the flexural toughness and impact resistance of steel fiber reinforced lightweight concrete and concluded that high compressive strength and density are desirable for good impact resistance of plain concrete. They also reported substantial improvement of impact resistance when steel fibers are incorporated [6]. Rao et al. investigated recycled aggregate concrete under drop-weight impact load and reported reduced impact resistance of recycled aggregate concrete with increasing percentage of recycled coarse aggregate [9]. Silica fume and steel fibers have also been reported to improve the performance of high strength concrete under impact, fatigue, and repeated dynamic loading, collectively and independently. The combined effect of silica fume and fibers are reported to be greater than the sum of their individual effect [7]. Gupta et al. replaced the fine aggregates by waste rubber fibers and cement by silica fume and studied impact resistance of concrete by drop-weight test, flexural loading test, and rebound test [8]. They demonstrated that, by replacing fine aggregates with rubber fibers and cement with silica fume, impact resistance and ductility can be improved. They also reported a good correlation among the results obtained by three different impact test methods.

In terms of impact testing, Marar et al. [11] developed a simple, economical drop-weight impact testing machine which dropped a larger mass (30 lb (13.5 kg)) than the method described by ACI committee 544 [12], to reduce the number of blows required, from a height of 1 ft (0.3 m) on a 6 in by 2.36 in (150 mm x 60 mm) disk, cut from 6 in diameter by 12 in height (150 mm x 300 mm) concrete cylinders. The specimens incorporated hooked-end steel fibers with three different aspect ratios (length/diameter) with four different fiber volume fractions up to 2.0%. At 28 days of age, their results showed that increased fiber content for all aspect ratios improved impact resistance. They also reported logarithmic relationship between compression toughness energy and impact energy [11]. Nili and Afroughsabet reported that number of blows at first crack and failure increase in specimens with polypropylene fibers [10]. Similarly, a lower w/c ratio leads to an increase in blows to failure, but at a slower rate. Silica fume in non-fibrous specimens' increases brittleness. Silica fume and fiber improves kinetic energy absorption capacity [10]. Rahmani et al. reported significant improvement of the first crack strength for cellulose and steel fiber reinforced concrete. While the post crack strength is not improved by the addition of cellulose fibers, it has remarkable effect on steel and polypropylene fiber reinforced concrete [2]. Song et al. reported slight improvement of impact strength of steel-polypropylene fiber reinforced concrete (SPHFRC) over steel fiber reinforced concrete (SFRC). Cracked SPFRC performs better than SFRC in post first crack region [13]. Lower maximum and residual deflection and better deflection recovery for UHPFRC is reported for a higher reinforcement ratio, reported by Yoo et al. [14]. They also concluded that at a certain drop height, the maximum crack width decreased with reinforcement ratio. In their study, a 595 lb (270 kg) drop-weight is allowed to freely fall from a drop height of 63 in (1600 mm) on large beams with dimensions 7.87 in by 10.63 in by 114.17 in (200 mm x 270 mm x 2900 mm) [14].

Researchers have adopted a variety of methods to evaluate the mechanical response of cementitious composites under high strain rate loads such as drop-weight test [15], pendulum impact test (Charpy test) [16], and split Hopkinson tension bar [17]. Although there are a number of impact loading methods that have been utilized, there are few corresponding testing standards that accompany those methods. One standard that does exist is the ACI standard, ACI 544.2R-89 Measurement of Properties of Fiber Reinforced Concrete. In this standard, the test is carried out by dropping a hammer with 10 lb (4.54 kg) mass from a height of 1.5 ft (45.7 cm). A 2.5 in (63.5 mm) diameter steel ball is centered on top of a disk shaped concrete specimen measuring 2.5 in (63.5 mm) thick with a 6 in (152 mm) diameter. The hammer is dropped by gravity force repeatedly and the number of blows to first crack and ultimate failure are recorded [12]. Statistical analysis has shown that the test results have high variation, requiring increased number of specimens to be tested to reach a reliable conclusion [18,19]. Additionally, it should be noted that this is only a relative test useful for comparing different concrete mixtures.

A modified version of ACI 544.2R is developed by Badr and Ashour [20] who sought to reduce the variability in the results of the test. They identified the following sources of scatter in results: allowing cracks to form anywhere and any direction, use of a single point of impact, variation in specimen preparation method, and shortcoming on the definition of ultimate failure. Their suggested modifications are: using notched specimens to force the cracks occur in a predefined path, using a 2 in (50.8 mm) line of impact instead of a single point, and all specimens having similar surface. They also defined the ultimate failure as the specimen is separated completely in for halves before touching the lugs of the apparatus or the specimen touches two opposite lugs of the apparatus, whichever happens first. They suggested that the specimen cracking through the line of impact and the two notches as the only accepted pattern of failure. Instead of 2.5 in (63.5 mm) thick specimens, they adopted a 2 in (50.8 mm) thick specimen. In this manner, coefficients of variation were reduced from 50-60% for the ACI 544 method to 35-40% for the modified method [20]. Other variations of drop-weight machine have also been used [14,15].

Damage accumulation under repeated impact load is poorly understood. Specifically, the additive properties of damage under multiple sub-critical impacts are unknown, and it is not currently possible to correlate the critical impact strength to the number of sub-critical impacts that lead to failure. Furthermore, testing under the current methodology results in results with high variability in results and with limited applicability of the results other than to compare different mix designs at the same singular impact energy, thus making it a relative and qualitative test. This research aims to improve upon the current methodology by testing specimens at multiple impact energies. Using multiple impact energies, an impact fatigue curve can be developed that can be used to identify the impact endurance limit and prediction of ultimate impact energy from an incomplete data set. Furthermore, by calculating the area under impact fatigue curve, a quantitative value for impact toughness can be obtained thus providing a better mechanical descriptor of the concrete mix. This paper presents this methodology by comparing three fiber reinforced concrete mixes' response to a prescribed energy impact testing regimen.

## EXPERIMENTAL METHODOLOGY

Damage accumulation curves for three fiber-reinforced concretes are obtained by measuring the number of blows to first crack and ultimate failure. The concrete mix proportions are shown in Table 1. The three fiber types used in this study are: a twisted steel fiber 1.0 in (25.4 mm) in length (Fiber 1), a virgin copolymer and recycled polypropylene blend macro-monofilament fibrillated fiber of 0.75 in (19.05 mm) in length (Fiber 2), and a monofilament polypropylene of 0.75 in (19.05 mm) in length (Fiber 3). The properties of the fibers are shown in Table 2 and an image of each is shown in Figure 1. For each mix, five specimens are prepared and tested for each drop height and the average and standard deviation of the five results are calculated. The specimens are cast into cylindrical molds and left to cure for 24 hours. The specimens are then demolded and cured in lime bath in a humidity-controlled chamber for 13 days.

**Table 1 - Concrete Mix Proportions**

| Material | Weight | | | | Specific Gravity |
|---|---|---|---|---|---|
| Coarse Agg. | 1816 | lb/yd$^3$ | (1077.39 | kg/m$^3$) | 2.75 |
| Fine Agg. | 1201 | lb/yd$^3$ | (712.52 | kg/m$^3$) | 2.65 |
| Cement | 646 | lb/yd$^3$ | (383.26 | kg/m$^3$) | 3.15 |
| Fly Ash | 114 | lb/yd$^3$ | (67.63 | kg/m$^3$) | 2.45 |
| Water | 279 | lb/yd$^3$ | (165.52 | kg/m$^3$) | 1 |
| Plasticizer | 11 | fl oz/yd$^3$ | (425.5 | ml/m$^3$) | 0.98 |
| Fiber | 7.5 | lb/yd$^3$ | (4.45 | kg/m$^3$) | 0.91-7.8 |

**Table 2 - Fiber Characteristics**

| | Fiber 1 | Fiber 2 | Fiber 3 |
|---|---|---|---|
| Fiber Type | Twisted steel wire | Macro-monofilament/ fibrillated-net blend | Monofilament Polypropylene |
| Specific Gravity | 7.8 | 0.91 | 0.91 |
| Tensile Strength | 246.5 ksi (1.7 Gpa) | 83-96 ksi (0.57-0.66 Gpa) | 25 ksi (0.17 Gpa) |
| Length | 1.0 in. (25.4 mm) | 0.75 in. (19 mm) | 0.75 in. (19 mm) |
| Nominal Diameter | 0.02 in. (0.5 mm) | 0.02 in. (0.5 mm) | 7 deniers |

**Figure 1 - Fiber Types (from left to right) Fiber 1, Fiber 2, and Fiber 3**

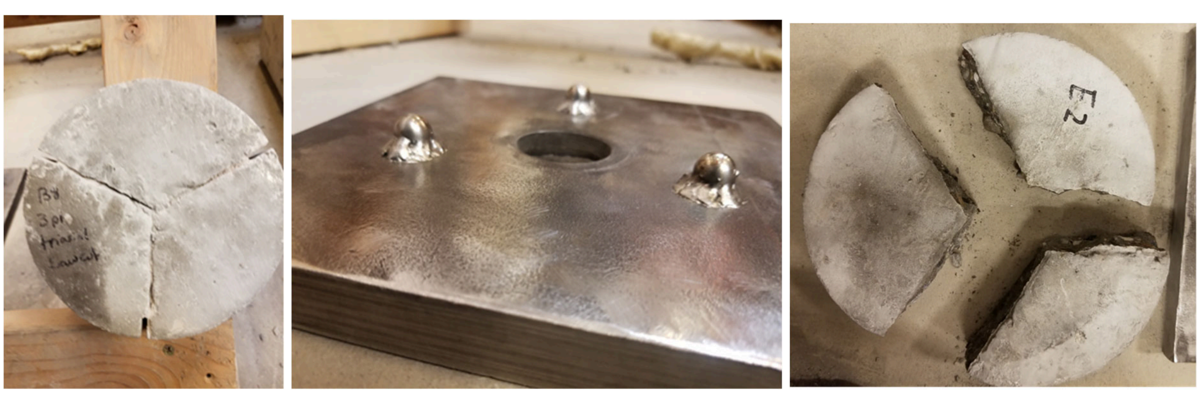


**Figure 2 - (a) Typical grooved disk specimen, (b) steel plate with support balls, (c) typical failure mode**

In a parametric study parallel to this study, an optimum specimen size and preparation methodology are developed. It is determined from that study that an optimum disk specimen of 2 in by 6 in (50.8 mm by 152.4 mm) be used. To prepare the specimens, molds of appropriate size are made. Fresh concrete is poured into the molds, rodded 25 times, and then the top surfaced is levelled with a trowel. Additionally, the specimens are grooved on the top with the help of a trowel such that the specimen is split into three equal parts (see Figure 2(a)). The specimens are covered with plastic sheet until demolding. After 24 hours, the specimens are demolded and stored in a curing chamber for 27 days. By prepping the specimens in this manner, a more consistent, controlled failure mode is achieved which provides increased accuracy and comparison between specimens (see Figure 2(c)). The specimens are set on a steel plate with three 0.5 in (12.7 mm) diameter welded steel balls at 120° radial spacing. The balls are placed on the diameter of a 5-in (127 mm) circle such that there is 1 in (25.4 mm) clear spacing between the outside of the specimen and the supporting balls (see Figure 2(b)). This support condition is similar to the ball-on-three balls (B3B) biaxial flexure test. The specimens are aligned such that the failure planes (groove locations) are offset 60º from the balls. Once the specimen is placed on the plate, a 3 in (76.2 mm) diameter, hardened steel ball is placed on the top center of the specimen. This hardened ball is held in place such that the impact point is continuous throughout the testing. It should be noted that the frame does not prevent impactor rebounding. The testing setup is shown in Figure 3.

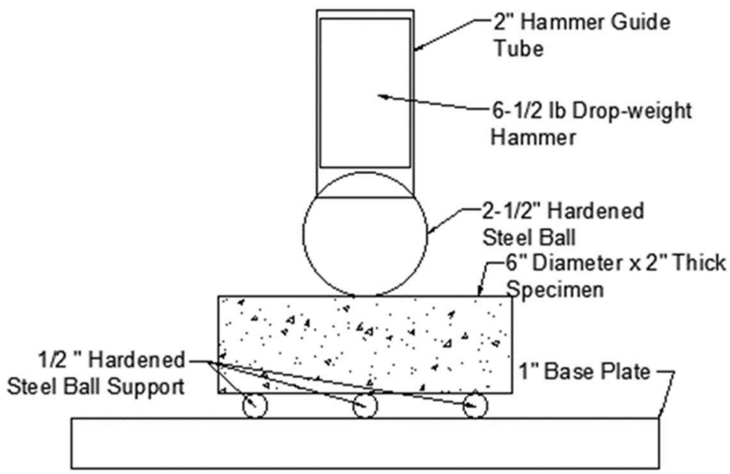


**Figure 3 - Drop weight test setup**

Using a constructed drop machine (Figure 4), a 6.5 lb (3 kg) hammer is dropped from heights of 1.5, 2, 3, 4, and 5 ft (457.2, 609.6, 914.4, 1219.2, and 1524.0 mm). The number of drops from each height is counted for both the first noticeable crack and ultimate failure according to ACI 544. During each specimen's test cycle, the hammer is raised to the specified drop height and released allowing it to freely impact the hardened steel ball. The etched failure plane of the specimen is placed on the bottom during testing. This is done to ensure that the failure would localize in the predefined path during the split second of tension on the bottom surface developed during impact. This process is repeated until a noticeable crack appears on the specimen. The number of blows is then recorded. The test resumes until the specimen reaches ultimate failure. The number of blows is then recorded. Ultimate failure is defined as a crack that completely breaks through the specimen and fiber bond displacing the specimen into two or more pieces. After all the specimens of the group are tested, the groups mean blow counts, standard deviation, and coefficient of variation (COV) are calculated.

**Figure 4 - Drop weight apparatus**

## ANALYTICAL METHODOLOGY

The experimental methodology described in the previous section is used to correlate the impact life (number of blows $N$) to the impact energy $E$ in what the authors term an impact fatigue curve. This moniker relates to the similarities between the repeated impact test method proposed here and the fatigue test method used for metals. The impact fatigue curve is expected to closely resemble the stress-life ($S - N$) curve originally developed by Wohler, which correlates the fatigue life (number of cycles $N$) to the fully reversed stress level $S$ under tensile fatigue [21–23]. An example $S - N$ curve is shown in Figure 5. The impact fatigue curve will be of much higher utility than the number of cycles to failure under a single repeated impact energy. First, it is anticipated that the critical impact condition can be extrapolated from the impact fatigue curve by finding the point at which the number of cycles to failure approaches unity ($N \to 1$). It is further anticipated that the number of cycles to failure under an impact condition that is not directly tested can be predicted by interpolation within the sample space or by extrapolation outside the sample space.

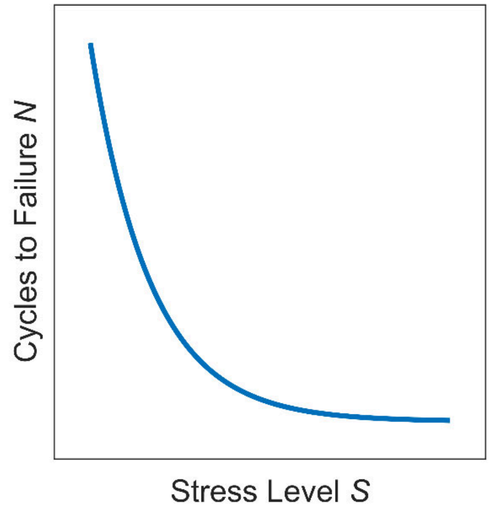


**Figure 5 - Fatigue curve (S-N or Wohler curve) relating life cycle *N* to stress level *S* under fully reversed cyclic tension**

## RESULTS

Using the methodology previously presented, the testing for the three fiber concrete mixes is carried out. The statistics on the results of the testing are shown in Table 3 which shows the mean number of blows to first crack and ultimate failure. During the testing, the first crack for the fiber reinforced concrete mixes is difficult to ascertain. As such, more consideration is given to the ultimate failure than first crack. Using the mean blows to ultimate failure, and by converting the drop height to impact energy, the values from Table 3 are plotted for each fiber mix at each impact energy and shown in Figure 6. The resulting curves follow the expected pattern; as the drop height or impact energy increase, the number of blows to ultimate failure decreases. Fibers 1 and 2 exhibit very similar behavior at all drop heights. Fiber 3 however, performed better at the lower impact energies but worse at the higher energies. The performance of Fiber 3 at the higher impact energies is not unexpected when the fiber tensile capacities of the fibers are considered. The tensile capacity of Fiber 3, 25,000 psi (170 MPa), is significantly lower than that of Fibers 1 and 2.

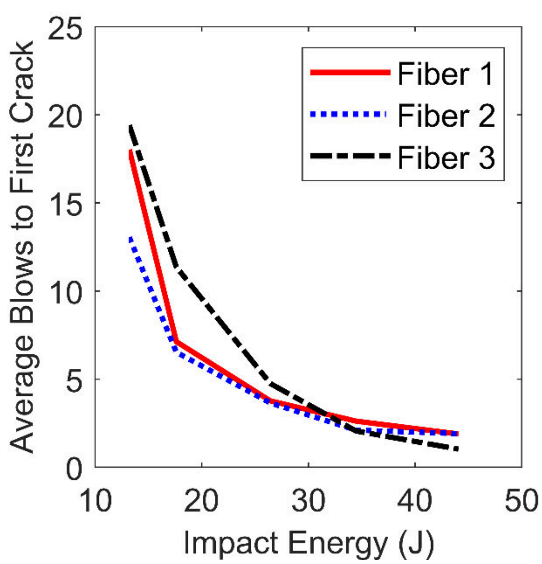


(a)

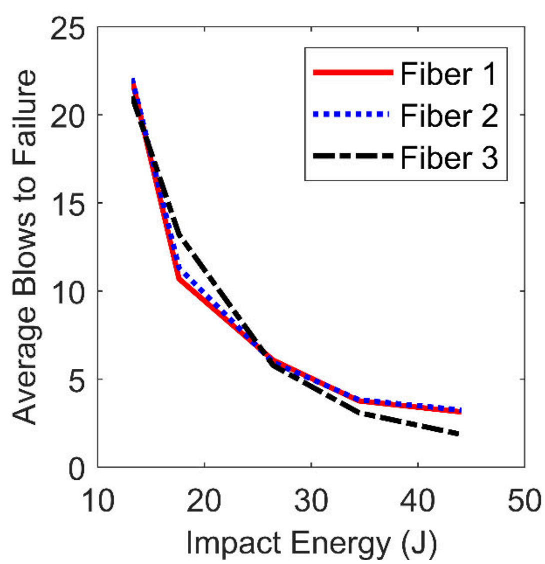


(b)

**Figure 6 - Number of blows to (a) first crack and (b) failure; average of 5 specimens each (1 Joule = 0.7376 feet-pound)**

**Table 3 - Number of blows to first crack and ultimate failure**

| Drop Height | | Fiber 1 | | Fiber 2 | | Fiber 3 | |
|---|---|---|---|---|---|---|---|
| | | First Crack | Ultimate Failure | First Crack | Ultimate Failure | First Crack | Ultimate Failure |
| 1.5 ft (0.15 m) | Mean Blows | 18.03 | 22.01 | 13.05 | 22.07 | 19.41 | 21.06 |
| | Standard Deviation | 6.60 | 8.55 | 7.33 | 8.50 | 4.92 | 4.93 |
| | COV | 36.63% | 38.83% | 56.14% | 38.52% | 25.34% | 23.41% |
| 2.0 ft (0.61 m) | Mean Blows | 7.13 | 10.69 | 6.53 | 11.32 | 11.36 | 13.21 |
| | Standard Deviation | 1.55 | 2.27 | 2.99 | 3.21 | 1.46 | 1.70 |
| | COV | 21.81% | 21.25% | 45.80% | 28.36% | 12.86% | 12.84% |
| 3.0 ft (0.91 m) | Mean Blows | 3.77 | 6.08 | 3.65 | 5.95 | 4.75 | 5.78 |
| | Standard Deviation | 1.20 | 1.72 | 1.42 | 1.72 | 0.92 | 0.09 |
| | COV | 31.67% | 28.33% | 39.03% | 28.85% | 19.44% | 15.97% |
| 4.0 ft (1.22 m) | Mean Blows | 2.62 | 3.77 | 2.11 | 3.83 | 2.06 | 3.10 |
| | Standard Deviation | 1.05 | 1.20 | 0.43 | 0.67 | 0.00 | 0.00 |
| | COV | 40.00% | 31.67% | 20.33% | 17.68% | 0.00% | 0.00% |
| 5.0 ft (1.52 m) | Mean Blows | 1.89 | 3.14 | 1.91 | 3.25 | 1.03 | 1.86 |
| | Standard Deviation | 0.47 | 0.07 | 0.00 | 0.52 | 0.00 | 0.46 |
| | COV | 24.85% | 23.57% | 0.00% | 16.11% | 0.00% | 24.85% |

Using the curves generated in Figure 6, the values for blow counts can be extrapolated to other impact energies. As with any empirical relationship, the accuracy of interpolation and extrapolation depend on a robust and representative sample space. Thus, extrapolation outside the bounds of testing cannot be considered reliable. In particular, the end points of the impact fatigue curve are not well defined due to the limitations of the testing program. Theoretically, the critical impact energy, which results in instantaneous failure, can be found by extrapolating to the value of impact energy at $N = 1$. However, the discrete nature of the number of blows, especially at small blow counts, renders this extrapolation problematic. Direct experimentation around small values of $N$ can improve the definition of the critical impact energy and the entire impact fatigue curve. Extrapolation outside the upper bounds of the impact fatigue curve is similarly problematic. Improved definition of the upper tail of the impact fatigue curve is experimentally challenging since it requires the operator to apply a very large number of very small blows. A simple corollary can be drawn to low cycle versus high cycle fatigue in metals. Low cycle fatigue experiments can be performed quickly, while high cycle fatigue experiments often take several days to complete.

Additionally, the area under each curve can be calculated. This is similar to calculating the toughness of a material by taking the area under the stress-strain curve. This area is hereafter referred to as the energy absorption index value ($\xi$) and can be used as one criterion for practitioners wishing to specify a mix that have good resilience over a range of impact energies. The index for each of the fiber mixes is calculated and shown in Table 4. As all three fiber mixes performed relatively equal, the index is approximately equal as well. While in this particular case the results don’t necessarily provide an indicative favorite, this criterion is just one of many that a designer would use to select a fiber mix. Additionally, no discussion is presented here on other facets of performance such as long-term durability or on economic advantages of the fibers. The purpose of this experiment is to show the application of the developed method for gaining a broader perspective of the performance of concrete mixes under a range of impact energies.

**Table 4 - Area under the drop impact failure curve (energy absorption index (ξ))**

| Fiber No. | Index |
|---|---|
| 1 | 217.65 |
| 2 | 223.83 |
| 3 | 218.60 |

## CONCLUSIONS

From the results of the testing, the following conclusions are made:

1. An impact fatigue curve can be generated from repeated impact tests of similar specimens with varying drop heights and/or impact energies. The impact fatigue curve, which is analogous to the stress-life curve in fatigue testing, relates the number of blows to failure (N) to the impact energy. The impact fatigue curve can be used to predict the critical impact condition (N=1) by extrapolation or to predict the impact fatigue life for impact energies not tested by either interpolation or extrapolation.
2. The ACI 544-89 impact test is not an active standard. Since there is no standardized test method for dynamic testing of concrete, derivations of this test continue to be used in contemporary research. An updated, codified standard should be developed that includes multiple impact energies. The results can then be plotted to produce an impact fatigue curve that can be used to extrapolate to other energies and to determine the energy absorption index.
3. With the absence of fiber reinforcement, the first crack impact resistance is difficult to detect. This makes data analysis for the first crack ambiguous and as such should be excluded.
4. The area under the curve of the impact fatigue curve can serve as an estimate of impact absorption in terms of an energy absorption index. This index is useful to design engineers in selecting concrete mixtures for structures that are subject to impact loading.